PROCEEDINGS OF SCIENCE

The VLBI imaging survey of the 6.7 GHz methanol masers using the JVN/EAVN

K. Sugiyama[*a], K. Fujisawa[ba], K. Hachisuka[c], Y. Yonekura[d], K. Motogi[b], Z. -Q. Shen[c], M. Honma[e], T. Hirota[e], S. Sawada-Satoh[f], Y. Murata[g], A. Doi[g], R. Dodson[h], M. J. Rioja[h], S. P. Ellingsen[i], K.-T. Kim[j], and H. Ogawa[k]

[a] *Graduate school of Science and Engineering, Yamaguchi University, Japan*
[b] *Research Institute for Time Studies, Yamaguchi University, Japan*
[c] *Shanghai Astronomical Observatory, Chinese Academy of Sciences, China*
[d] *Center for Astronomy, Ibaraki University, Japan*
[e] *VERA Project, National Astronomical Observatory of Japan (NAOJ), Japan*
[f] *Mizusawa VLBI Observatory, NAOJ, Japan*
[g] *The Institute of Space and Astronautical Science, Japan Aerospace Exploration Agency, Japan*
[h] *International Center for Radio Astronomy Research, University of Western Australia, Australia*
[i] *School of Mathematics and Physics, University of Tasmania, Australia*
[j] *Korea Astronomy and Space Science Institute, 776 Daedeokdae-ro, South Korea*
[k] *Department of Physical Science, Osaka Prefecture University, Japan*
E-mail: koichiro@yamaguchi-u.ac.jp

We present a result of the VLBI imaging survey for the 6.7 GHz methanol masers by using the Japanese VLBI Network (JVN) and the East-Asian VLBI Network (EAVN). We conducted VLBI observations for 36 methanol maser sources, in which 22 sources and another 14 sources were observed in August 2010 and November 2011, respectively. In all target sources, the spatial distribution of 35 sources were obtained, in which 33 sources provide new VLBI images. The spatial morphology was classified into five categories (elliptical, arched, linear, pair, and complex) on the basis of the criteria used in the European VLBI Network (EVN) observations [1]. In the EAVN 36 target sources, 24 sources except for near equatorial sources ($-5 <$ Dec $< +5$ deg) were also observed by using the Australia Telescope Compact Array (ATCA) to obtain spatial morphology of the 6.7 GHz methanol masers without the missing flux. The ATCA images detected new maser spots, which could be inferred as being resolved out on the JVN/EAVN images, and resolved an ambiguity of the complex spatial morphology in three sources.

11th European VLBI Network Symposium & Users Meeting,
October 9-12, 2012
Bordeaux, France

[*] Speaker.

PoS(11th EVN Symposium)032

1. Introduction

The process through which high-mass star form has been a matter of debate for many years. But in the last decade, high-resolution interferometric observations at submillimeter and infrared wavelengths have demonstrated the existence of rotating disks around high-mass young stellar objects (HMYSOs) (e.g., [2, 3]). For the next studies, the evolution of the disk around HMYSOs must be understood by a combination of Very Long Baseline Interferometer (VLBI) and the Atacama Large Millimeter/Submillimeter Array (ALMA) observations. Studies of the proper motion of individual compact maser spots with VLBI are the only tools to directly provide information about the rotation and/or the infall motions of the disk on scales of a few milliarcsecond per year (mas yr^{-1}).

The methanol maser transition at 6.7 GHz can be the best probe for investigations of HMYSOs, on the basis of characteristics such as the detection of this maser only in high-mass star-forming regions, a long lifetime, and their coming up before forming an ultra-compact HII region. Furthermore, methanol masers are thought in some cases to be associated with the rotating disk around HMYSOs, on the basis of their spatial morphology and radial-velocity gradient (e.g., [4]). More recently, Bartkiewicz et al. (2009) [1] observed nine out of 31 sources ($\sim$30%) with a ring-like morphology using the EVN. They investigated various scenarios with rotating and expanding disks and noted that in general the expansion/inflow velocity was higher than the rotation component. These results will be demonstrated by measuring relative proper motions, as done for some sources, giving some clues about the nature of the high-mass star formation (e.g., [5, 6, 7]).

We have started a VLBI monitor project of the methanol maser sources at 6.7 GHz using the JVN and the EAVN to systematically measure the relative proper motions for more than 30 sources since 2010. In this proceeding, we present a result of the VLBI imaging survey for the methanol masers observed during the 1st epoch observations in 2010/2011. Also, we show a comparison with the ATCA results of the 6.7 GHz methanol masers without the missing flux, which were obtained in 2012.

2. Observations

2.1 JVN/EAVN

The target methanol maser sources at 6.7 GHz were selected from the methanol maser catalog [8] and the Methanol Multibeam Survey catalog published in 2010 [9, 10] using the following criteria: 1) The source declination is $> -40^{\circ}$; 2) The total flux densities are > 65 Jy in either catalog; 3) There is no past VLBI observation. Applying these criteria, 34 sources were selected and other two sources were included for the verification of imaging capabilities, as listed in table 1. Almost all the target sources (34/36, 94%) were located in southern hemisphere (Dec $< 0^{\circ}$), implying that they were also observable using the ALMA.

We used six (Mizusawa, Iriki, Ogasawara, Ishigaki, Hitachi, and Shanghai) and seven/eight (the previous six and/or Yamaguchi, Usuda) radio telescopes of the JVN/EAVN in August 2010 and November 2011, respectively. All the telescopes used a left-hand circular polarization observing mode. The projected baselines ranged from 6 Mλ to 50 Mλ corresponding to fringe spacings of 34.4 mas and 4.1 mas at 6.7 GHz. The observations were made using a snapshot mode, and the

Table 1: Summary of observed sources.

G-Name	RA(J2000) (^{h} ^{m} ^{s})	Dec(J2000) ($^{\circ}$ $'$ $''$)	V_{lsr} (km s^{-1})	F_p (Jy)	Reference	ATCA
00.546−0.852	17 50 14.35	−28 54 31.1	11.8	68.0	c10	AT
00.645−0.042	17 47 18.67	−28 24 24.8	49.1	69.0	c10	AT
02.536+0.198	17 50 46.47	−26 39 45.3	3.1	88.0	c10	AT
06.189−0.358	18 01 02.16	−23 47 10.8	−30.2	228.6	g10	AT
06.795−0.257	18 01 57.75	−23 12 34.9	16.3	91.1	g10	AT
08.683−0.368	18 06 23.49	−21 37 10.2	43.2	102.0	g10	AT
08.832−0.028	18 05 25.67	−21 19 25.1	−3.8	159.1	g10	AT
09.619+0.193	18 06 14.92	−20 31 44.3	5.5	70.0	g10	AT
09.986−0.028	18 07 50.12	−20 18 56.5	42.2	67.6	g10	AT
10.323−0.160	18 09 01.46	−20 05 07.8	11.5	90.1	g10	AT
11.497−1.485	18 16 22.13	−19 41 27.1	6.6	68.4	g10	AT
11.904−0.141	18 12 11.44	−18 41 28.6	42.9	65.0	g10	AT
12.025−0.031	18 12 01.86	−18 31.55.7	108.3	96.3	g10	AT
12.681−0.182	18 13 54.75	−18 01 46.6	57.5	544.0	g10	AT
12.889+0.489	18 11 51.40	−17 31 29.6	39.3	68.9	g10	AT
14.101+0.087	18 15 45.81	−16 39 09.4	15.4	87.3	g10	AT
20.237+0.065	18 27 44.56	−11 14 54.2	71.8	77.0	c09	AT
23.437−0.184	18 34 39.25	−08 31 38.5	103.0	77.0	c09	AT
25.650+1.050	18 34 20.91	−05 59 40.5	41.9	178.0	x09	
25.710+0.044	18 38 03.15	−06 24 15.0	92.8	364.0	x09	AT
25.826−0.178	18 39 03.63	−06 24 09.5	91.2	70.0	x09	
28.832−0.253	18 44 51.09	−03 45 48.0	83.5	73.0	x09	
29.86−0.04	18 45 59.57	−02 45 04.4	101.4	67.0	x09	
30.704−0.068	18 47 36.9	−02 01 05.	88.0	87.0	x09	
30.760−0.052	18 47 39.73	−01 57 22.0	92.0	68.0	x09	
30.91+0.14	18 47 15.0	−01 44 07	104.0	95.2	x09	
31.282+0.062	18 48 12.39	−01 26 22.6	110.0	71.0	x09	
32.050+0.059	18 49 37.3	−00 45 47	92.8	93.0	x09	
37.40+1.52	18 54 10.5	+04 40 49	41.1	279.0	x09	
49.490−0.388	19 23 43.949	+14 30 34.44	59.2	850.0	x09	
232.621+0.996	07 32 09.79	−16 58 12.4	23.0	162.0	c09	
351.775−0.536	17 26 42.57	−36 09 17.6	1.3	231.0	c10	AT
352.630−1.067	17 31 13.91	−35 44 08.7	−2.9	183.0	c10	AT
353.410−0.360	17 30 26.18	−34 41 45.6	−20.3	116.0	c10	AT
354.615+0.472	17 30 17.13	−33 13 55.1	−24.4	166.0	c10	AT
359.436−0.104	17 44 40.60	−29 28 16.0	−47.8	73.5	c10	AT

Column 1: Galactic name; Column 2, 3: Absolute coordinates used in our observations; Column 4, 5: Radial velocity and flux density of the brightest maser feature; Column 6: Reference for the absolute coordinate; Column 7: Marked by “AT" in the case that the ATCA observations were also conducted. Reference – c09[11]; x09[12]; c10[9], g10[10].

integration time was set as 3 to 4 15-minute scans for each source, spaced over a period of 9 hr. The typical image noise rms was 30-50 mJy beam^{-1}. The data were calibrated using AIPS [1].

2.2 ATCA

The ATCA observations were conducted in February 2012 for 24 sources after excluding near equatorial sources ($-5 <$ Dec $< +5$ deg) from the EAVN targets, as listed in table 1. We made observations at two frequency bands: 4.8-6.8 and 8.0-10.0 GHz, with both linear polarizations. Two recording sets on back-end system were used simultaneously as 2 GHz $\times$ 2IFs bandwidth for continuum, and 1 MHz bandwidth with 2048 ch $\times$ 8IFs for maser observations, which yielded a velocity resolution of 0.022 km s^{-1}. In this proceeding, however, a result of the continuum data set would not be shown. The array configuration was 6A, which implies a spatial resolution of $\sim 2.0 \times 1.5$ arcsec^2 at 6.7 GHz. The typical maser image noise rms was $\sim$100 mJy beam^{-1} with an integration time of $\sim$2.5 hr per source. The data were calibrated using Miriad [2].

3. Results & discussion

3.1 JVN/EAVN

We successfully obtained the spatial distribution of the 6.7 GHz methanol maser spots for 35 sources except for G14.101+0.087, for which fringes were only detected for one baseline formed by Mizusawa and Hitachi telescopes. For our sample, we provide new VLBI images for 33 sources, increasing by a factor of 1.5 the number of 6.7 GHz VLBI images of methanol masers. The spatial morphology of the imaged masers was classified into five categories: elliptical, arched, linear, pair, and complex, on the basis of the criteria used in the EVN observations [1]. The classification in the JVN/EAVN images is summarized in table 2.

Here, we present the JVN/EAVN images of the 6.7 GHz methanol maser spots in G00.546$-$0.852 and G06.795$-$0.257, which were classified into the elliptical spatial morphology category, as shown in figure 1. The least-square fitted ellipse to the maser distribution shows a diameter of a few thousand AU at the given source distances. A clear radial-velocity gradient in counterclockwise direction, in particular for G06.795$-$0.257, could be seen on the maser ellipse. The elliptical sources can be associated with a rotating disk, in some cases with expansion/infall components suggested by an EVN observation [1]. All the JVN/EAVN images and the classification of their spatial morphology will be published in Fujisawa et al. (submitted).

3.2 ATCA

The ATCA observations provided the spatial distributions of the 6.7 GHz methanol masers for the 24 target sources. The cross-power spectra represented over 90% of flux densities on total-power spectra for all targets, leading us to obtain a correct classification of the spatial morphology without the missing flux. The relative-positional errors were typically better than 100 mas, which was enough to define the spatial morphology extended wider than 300 mas. Here, we present the ATCA image obtained for G02.536+0.198 in figure 2. This source was already classified into the

[1] Software package used for astronomical data reductions developed at the National Radio Astronomy Observatory.
[2] Software package used for interferometric data reductions initiated by the Berkeley Illinois Maryland Association.

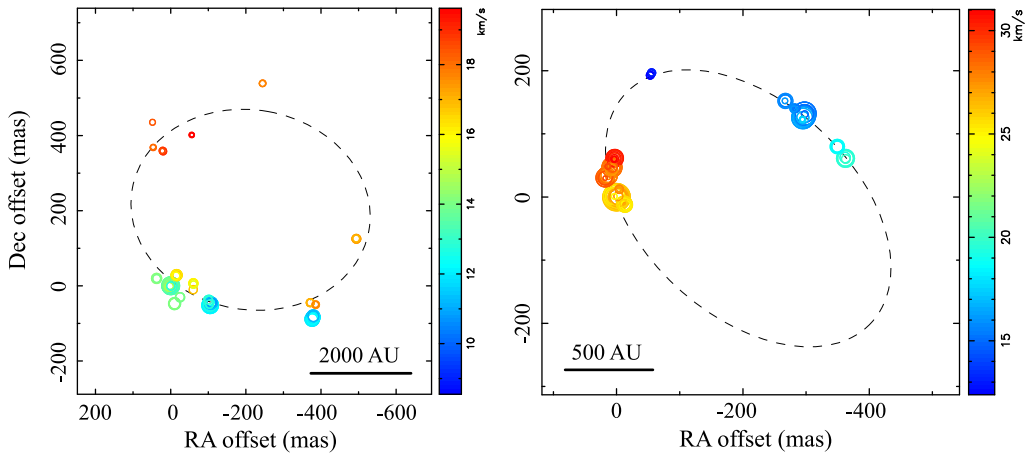

Figure 1: The JVN/EAVN images of the 6.7 GHz methanol maser spots in G00.546−0.852 (left) and G06.795−0.257 (right). The spot size and color indicate its peak intensity in logarithmic scale and its radial velocity (see color index at the right-hand side), respectively. The origin of the map corresponds to the absolute coordinate described in table 1. The dashed ellipse shows the least-square fit on the maser spatial distribution.

elliptical morphology category on the basis of the JVN/EAVN image. The ATCA image made it clearer with the detection of new maser spots in the north-west direction. The new maser spots could be inferred as being resolved out on the JVN/EAVN image since in some cases the spots had an extension size larger than 100 AU like a halo component [13].

The spatial morphology was re-classified into the five categories on the basis of the ATCA images, as listed in table 2. We could resolve an ambiguity of the complex three sources by detecting also the halo components, and then increase elliptical sources. These results suggest that a collaboration of VLBI and connected array, such as the ATCA, observations is important to determine the spatial morphology and the associated site of the methanol masers. These will be demonstrated by measuring masers proper motions using the JVN/EAVN in the near future.

Table 2: The classification of the spatial distribution for the 6.7 GHz methanol maser spots.

Array	Spatial morphology				
	Elliptical	Arched	Linear	Pair	Complex
JVN/EAVN	6	3	6	6	14
JVN/EAVN for ATCA†	5	2	2	4	10
ATCA‡	9	1	2	4	7

†: Target sources observed using both the JVN/EAVN and the ATCA.

‡: Exclude the source G14.101+0.087, which was resolved out in the JVN/EAVN.

References

[1] A. Bartkiewicz, et al., *The diversity of methanol maser morphologies from VLBI observations*, 2009, A&A, 502, 155

[2] N. A. Patel, et al., *A disk of dust and molecular gas around a high-mass protostar*, 2005, Nature, 437, 109

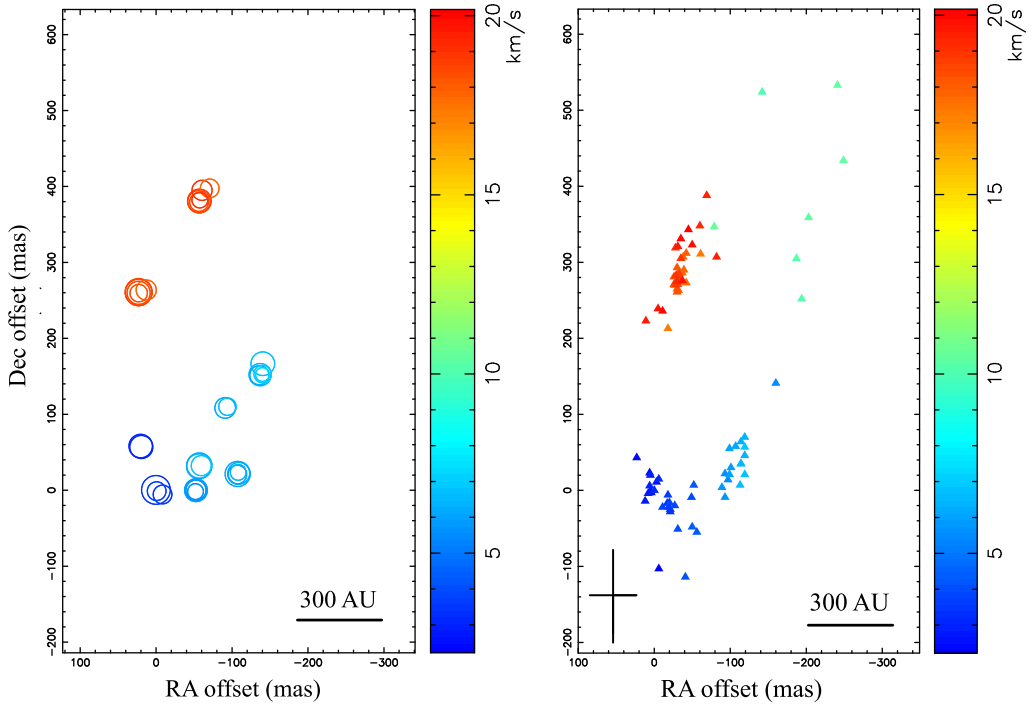

Figure 2: The spatial distribution of the methanol maser spots in G02.536+0.198. *Left*: JVN/EAVN image. The maser spots are shown by open circles with logarithmic scale depending on its peak intensity. *Right*: ATCA image. The maser spots are shown by triangles with fixed scale. The typical relative-positional error is shown at the bottom-left corner.

[3] S. Kraus, et al., *A hot compact dust disk around a massive young stellar object*, 2010, Nature, 466, 339

[4] R. P. Norris, et al., *Synthesis images of 6.7 GHz methanol masers*, 1993, ApJ, 412, 222

[5] A. Sanna, et al., *VLBI study of maser kinematics in high-mass star-forming regions. I. G16.59−0.05*, 2010a, A&A, 517, A71

[6] A. Sanna, et al., *VLBI study of maser kinematics in high-mass star-forming regions. II. G23.01−0.41*, 2010b, A&A, 517, A78

[7] C. Goddi, et al., *Infall and outflow within 400 AU from a high-mass protostar. 3D velocity fields from methanol and water masers in AFLG 5142*, 2011, A&A, 535, L8

[8] M. R. Pestalozzi, et al., *A general catalogue of 6.7-GHz methanol masers. I. Data.*, 2005, A&A, 432, 737

[9] J. L. Caswell, et al., *The 6-GHz methanol multibeam maser catalogue - I. Galactic Centre region, longitudes 345° to 6°*, 2010, MNRAS, 404, 1029

[10] J. A. Green, et al., *The 6-GHz methanol multibeam maser catalogue - II. Galactic longitudes 6° to 20°*, 2010, MNRAS, 409, 913

[11] J. L. Caswell, *Precise Positions of Methanol Masers*, 2009, PASA, 26, 454

[12] Y. Xu, et al., *Absolute positions of 6.7-GHz methanol masers*, 2009, A&A, 507, 1117

[13] V. Minier, et al., *VLBI observations of 6.7 and 12.2 GHz methanol masers toward high mass star-forming regions. III. The milliarcsecond structures of masing regions*, 2002, A&A, 383, 614